



Rapid Determination of the Fatigue Behavior at Different Stress Ratios of Steels by Measuring the Energy Release

Danilo D'Andrea , Eugenio Guglielmino , Giacomo Risitano ,
and Dario Santonocito  

Department of Engineering, University of Messina, Contrada di Dio Sant'Agata,
98166 Messina, Italy

dsantonocito@unime.it

Abstract. Structural integrity of mechanical devices is of fundamental importance for reliability under the action of service loads. To properly design a mechanical device against fatigue failure, a long test campaign involving many specimens and time must be performed according to traditional fatigue tests protocol. However, fatigue is a very dissipative phenomenon in which a large amount of energy is dissipated in the surrounding environment. Moving from this assumption, the adoption of infrared thermography can dramatically decrease the amount of time to obtain reliable information regarding the fatigue life of materials and components. Risitano Thermographic Method (RTM) links the superficial temperature during a fatigue test with the dissipated energy for a given stress level. The whole fatigue life of a specimen is represented by an Energy Parameter, strictly dependent on the test frequency and stress ratio, and this allow to obtain, even with one specimen, the entire fatigue curve. The Static Thermographic Method (STM) allows to assess the first damage in a specimen subjected to static tensile test by monitoring the superficial temperature evolution. The obtained limit stress could be directly related with the onset of fatigue damage within the material if cyclically stressed. The aim of the present work is to investigate the relation between the energy release and the damage at different stress ratios within a stainless steel AISI 316L, both under static tensile and fatigue tests using RTM and STM. Moreover, microstructure analysis is carried out to identify possible failure sites.

Keywords: Energy dissipation · Infrared thermography · Static Thermographic Method · Microstructure

1 Introduction

The assessment of the fatigue life of materials requires a very large number of specimens to break and time to perform all the tests. However, in the last thirty five years infrared thermography [1] has significantly changed the testing paradigm, shortening the required time. This is due to the intrinsic nature of the fatigue phenomenon which is highly dissipative, indeed a large amount of the mechanical work provided to the specimen

is converted into heat and exchanged with the surrounding environment [2]. The first researcher who monitored the superficial temperature of a specimen with an infrared camera was Risitano in 1984 [3]. Since 1984 several studies were performed by Risitano and co-workers [1], up to 2000 when the Risitano Thermographic Method (RTM) [4] was proposed as a test procedure to derive the fatigue properties of engineering material in a very rapid way. Nowadays it is possible to perform reliable tests by adopting affordable testing setup [5].

Other researchers also adopted thermography and other energy-based techniques to assess the fatigue properties of a wide class of materials, under several loads conditions [6–12]. In 2013 Risitano and Risitano proposed a rapid test procedure to assess the beginning of damage within the material monitoring the superficial temperature during a static tensile test [13], i.e. the Static Thermographic Method (STM). A limit stress could be identified when a deviation from the linear thermoelastic trend of the temperature signal is noticed. The Static Thermographic Method has been applied to several kind of materials and compared both with traditional fatigue tests and RTM, showing good agreement [7, 14–17].

Moving from the author's experience on the fatigue assessment of Additive Manufactured AISI 316L specimens [18], in this work, a comparison between the energy release of austenitic stainless steel AISI 316L specimens subjected to static tensile and stepwise fatigue tests, under two different stress ratio conditions, has been performed. The energetic release has been monitored and the fatigue limits by Thermographic Methods have been assessed and compared with literature data. Microstructural analysis has been performed to identify possible sites of failure.

2 Theoretical Background

2.1 Risitano Thermographic Method

The first researcher who monitored the temperature trend during a fatigue test was Risitano in 1984. As formalized in the work by La Rosa and Risitano [4], during a constant amplitude fatigue test performed with a stress level above the fatigue limit of the material, with a given stress ratio R and test frequency f , the superficial temperature of the specimens exhibits three different phases (Fig. 1a). In the first phase a rise in the temperature signal is noticed until, in the second phase, a stabilization temperature is reached. Finally, in the third phase, a very high temperature increment is noticed up to the specimen failure. The fatigue limit of the material, under a given stress ratio, can be identified as the first stress level at which the stabilization temperature is noticeably higher compared to the previous values. On the other hand, for stress level below the fatigue limit of the material noise or no significative temperature increment is noticed. It is possible to evaluate the Energy Parameter Φ as the subtended area of the temperature vs. number of cycle curve (ΔT -N), given the stress ratio and the test frequency. The higher the applied stress level, the higher the stabilization temperature; however, the Energy Parameter is almost constant. If we perform fatigue tests with a stepwise increase of stress level, it is possible to record the related different stabilization temperatures and assess the Energy Parameter of a specimen once it fails (Fig. 1b) [19]. In such way, given the fact that the Energy Parameter is constant, it is possible to assess the number

of cycles to failure for each stress level simply dividing the Energy Parameter for the related stabilization temperature. By knowing the $N-\sigma$ values, it is possible to obtain the complete SN curve of the material, even with one specimen.

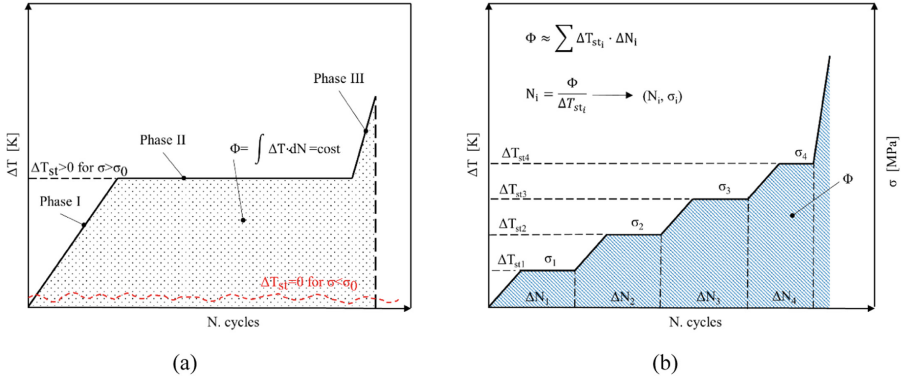


Fig. 1. a) Temperature evolution during a fatigue test; b) Temperature evolution during a stepwise fatigue test.

2.2 Static Thermographic Method

By observing the temperature evolution during a static tensile test, Risitano and Risitano in 2013 [13] proposed a very rapid procedure to assess the first damage within the material. The temperature evolution during a static tensile test is characterized by three phases (Fig. 2). In the first phase there is a linear decrease of the specimen temperature according to the thermoelastic effect and Lord Kelvin’s law (Eq. (1)). In the second phase the temperature trend exhibits the same linear decrement, with a different slope compared to the previous phase, until a minimum value of the temperature signal is reached. Finally,

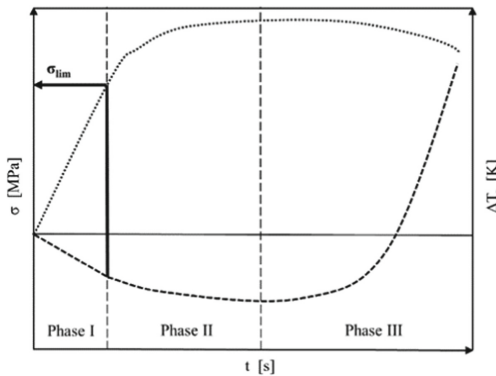


Fig. 2. Temperature trend during a static tensile test.

in the third phase temperature experience a very high further temperature increment due to the dissipative phenomena.

$$\Delta T_s = -K_m T \sigma_1 \quad (1)$$

By monitoring the superficial temperature of a specimen during a static tensile test, it is possible to define experimental stress vs. temperature vs. time diagram where the relation between the transition point from Phase I to Phase II can be identified and related to the first macroscopic stress that introduce in the material the first damage [20]. Such damage is able to activate sites of irreversible micro-plasticity within the material that would lead to fatigue failure if the material is cyclically loaded.

3 Materials and Methods

Static tensile and fatigue tests were performed on specimens produced according to ASTM E466 standard, with hourglass shape, under stress control with a servo hydraulic loading machine MTS 810 250 kN. The stress rate at which the static tensile tests were performed was 3 MPa/s, adopted in order to assure adiabatic test condition, i.e. the specimen must not be able to exchange heat with the surrounding environment. Stepwise fatigue tests were performed at two different stress ratio, $R = -1$ and $R = 0.1$, with a test frequency of $f = 10$ Hz (Fig. 3).

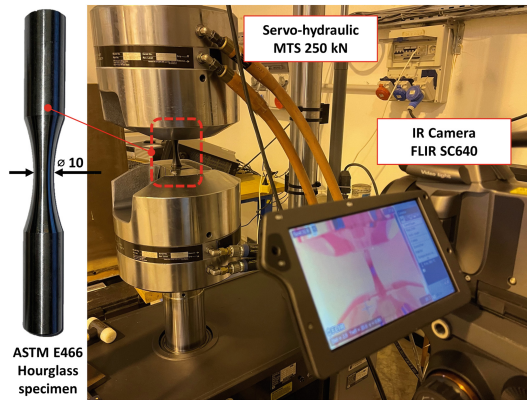


Fig. 3. Experimental test setup with the adopted specimen.

During the tests, the superficial temperature evolution of the specimen was monitored with an infrared camera FLIR SC640. The maximum value of a rectangular area, placed on the specimen surface, was recorded and filtered with a *rlowess* filter, with a data span of 5%, to exclude the outliers and enhance the temperature trend.

In order to characterize the microstructure of the AISI316L, failure analysis was performed using a LEICA stereomicroscope (LEICA Microsystems GmbH, Germany). Furthermore, the fracture surfaces were analyzed using a scanning electron microscope

(SEM) FEI Quanta 450 FEG (Thermo Fisher Scientific, Waltham, Massachusetts, US), operating at 20.00 kV in High Vacuum.

The composition of the alloy studied was obtained through XRF analysis, which confirmed the use of stainless steel AISI 316L as shown in Table 1.

Table 1. AISI316L chemical composition (in wt.%)

Mn	Cr	Mo	Ni	Cu	Fe
1.73	16.68	1.98	10.22	0.37	68.6

4 Results and Discussions

4.1 Static Tensile Test

Static tensile tests were performed on four specimens adopting a stress rate of 3 MPa/s. During the tests the superficial temperature of the specimen was monitored with the infrared camera. The nominal applied stress curve has been plotted respect the temperature (filtered signal) and time. As it is possible to observe from Fig. 4, the temperature signal exhibits a first linear decrease, due to the thermoelastic effect, followed by another linear decrease but with a different slope compared to the previous one.

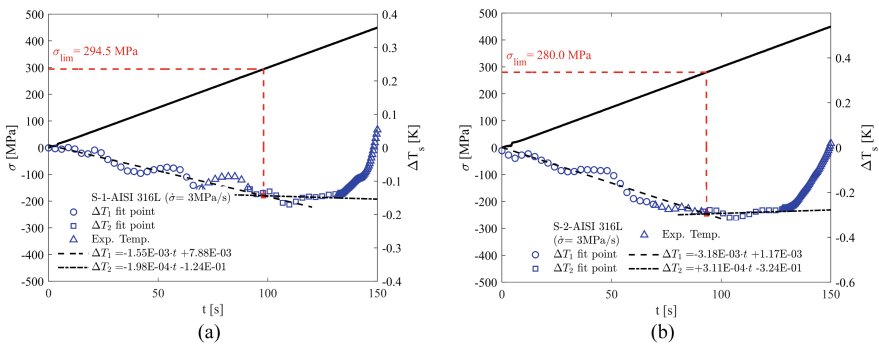


Fig. 4. Temperature trend vs. applied stress level during a static tensile test.

It is possible to make the linear regression of the two sets of temperature data (ΔT_1 and ΔT_2 fit points) and make their intersection. The corresponding stress level at the intersection can be assumed as the limit stress (σ_{lim}) for the specimen under investigation. For the four performed tests, an average value of $\sigma_{lim} = 282 \pm 15 \text{ MPa}$ has been obtained. The ultimate tensile strength is equal to $\sigma_U = 714 \pm 11 \text{ MPa}$, which is in good agreement with other literature data [21].

4.2 Stepwise Fatigue Test

Four fatigue tests, with a stepwise increase of the applied stress level were performed in order to monitor the energetic release of the material under cyclic loading conditions. Two tests have been performed adopting a stress ratio $R = -1$ and the remaining two with a stress ratio of $R = 0.1$. All the tests have been performed with a test frequency of $f = 10$ Hz and the infrared camera has been adopted to monitor the superficial temperature of the specimen.

In Fig. 5 have been reported the temperature trend vs. the applied stress level (σ_{sup} , maximum applied stress level) and number of cycles to failure for the different stress ratio. The applied stress level is the same for both the stress ratio; however, the tests performed at $R = -1$ exhibit a higher stabilization temperature compared to the tests performed at $R = 0.1$. As it is possible to observe from Fig. 5a for $R = -1$, a higher temperature increment is noticed between 290 MPa and 300 MPa. For the last two stress levels (320–330 MPa) it is not possible to observe a stabilization temperature, indeed the specimen fails. For the stepwise fatigue tests with $R = 0.1$ it has been possible to go beyond 330 MPa stress level, up to 600 MPa; however, for lower stress levels no increment or noisy signal has been noticed.

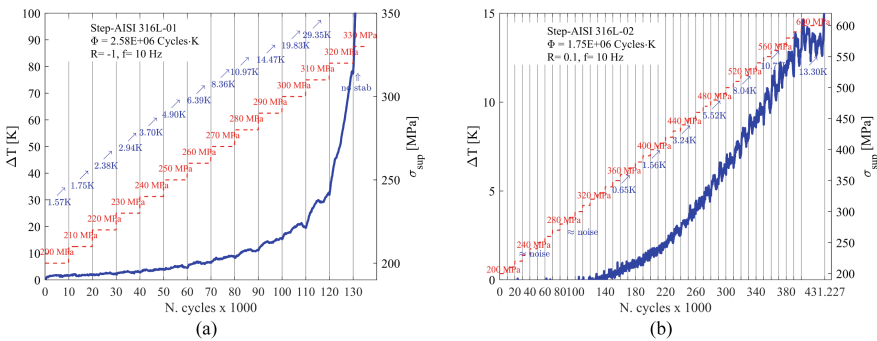


Fig. 5. Temperature evolution during stepwise fatigue tests performed at $f = 10$ Hz and stress ratio: a) $R = -1$; b) $R = 0.1$.

The Energy Parameter Φ has been evaluated as the integral of the temperature vs. number of cycles to failure curve, showing good agreement in terms of repeatability (2.58×10^6 and 2.68×10^6 Cycles K for $R = -1$; 1.64×10^6 and 1.75×10^6 Cycles K for $R = 0.1$). According to the previous considerations, given the higher temperature increment, for the same testing frequency and maximum applied stress level, the stress ratio $R = -1$ is the more damaging loading conditions for the material.

It is possible to assess the fatigue limit of the material for the different stress ratio conditions by reporting the different stabilization temperature vs. the maximum applied stress level (Fig. 6). The temperature points exhibit a bilinear trend, with a knee region where cyclic damage arises. By performing the linear regression of the two set of points and by making their intersection, it is possible to assess the fatigue limit for the two stress ratio loading conditions ($\sigma_{0,RTM} = 274$ MPa for $R = -1$, $\sigma_{0,RTM} = 434$ MPa).

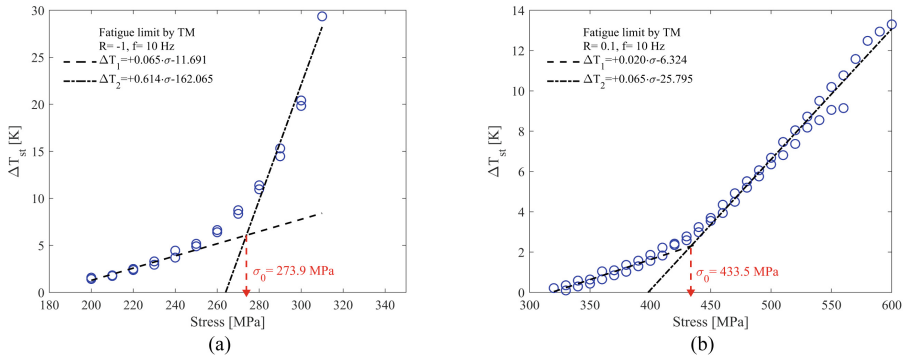


Fig. 6. Determination of the fatigue limit by the Thermographic Method for: a) $R = -1$; b) $R = 0.1$.

For the stress ratio of $R = -1$, some constant amplitude (C.A.) fatigue tests have been performed adopting the same testing frequency of 10 Hz. The run out (i.e. infinite life of the specimen) has been set at $N = 2 \times 10^6$ cycles. In Fig. 7 are reported the limit stress as assessed by the STM, the fatigue limit assessed by the RTM, the SN points from the RMT (blue circles), and other literature data. Huang et al. [22] tested some samples of AISI 316L undergoing to surface mechanical rolling treatment (SMRT-6, green hollow triangle) and strained SMRT specimen (T-SMRT-6, green full triangle) with 6 mm specimen diameter, at $R = -1$ and $f = 5$ Hz. Roland et al. [23] tested commercial AISI 316L specimen “as received” ($R = -1$, $f = 10$ Hz), while Peng et al. [24] tested carburized specimens ($R = -1$, $f = 15$ Hz). The CA fatigue tests performed in our study show three run outs for stress levels below 300 MPa and two failures for the stress level of 320 MPa, even with a high scatter. The SN points (four points) obtained by RTM exhibit the same trend of the data from Huang et al., which assess a fatigue limit of 320 MPa, and are in good agreement with other literature data.

In addition, the fatigue limit prediction of the Thermographic Methods are conservative compared to the CA run-out tests and with literature data (-11% for the STM; -14% for the RTM respect Huang et al.).

4.3 Failure Analysis

The fracture surfaces of specimens subjected to static tensile test was obtained by scanning electron microscope (SEM) analysis. As shown in Fig. 8, it is possible to highlight the typical cup-cone fracture surface characterized by the existence of the dimple-like

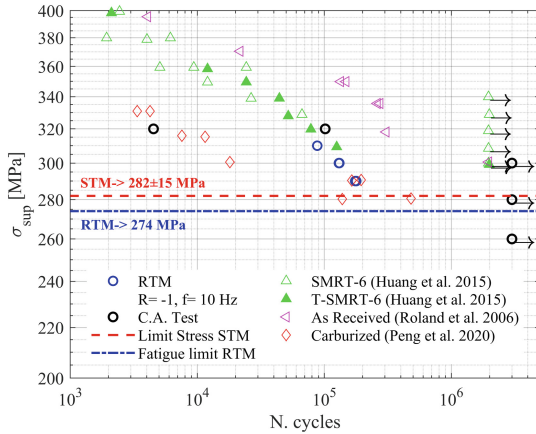


Fig. 7. Comparison of fatigue data for $R = -1$.

parabolic structures typical of ductile fracture mode. In particular, in Fig. 8b, at high magnification, it is possible to observe the austenitic morphology of the fracture surface.

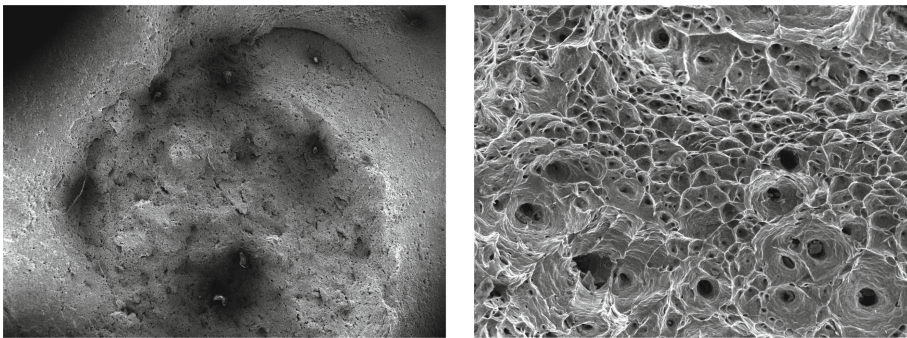


Fig. 8. SEM microscopies of AISI 316L static fracture surface. a) magnification of 100x; b) magnification of 4000x.

As shown in Fig. 9, the fatigue fracture surfaces are composed of different phases: crack initiation, crack growth zone, transition zone and brittle crack.

As underlined by the micrographs obtained with a scanning electron microscope at high magnification, the nucleation of the crack occurs close to the surface, at inclusions, and propagates inwards, leaving a distinct region of crack propagation that appears as grooves or streaks (Fig. 9a). Figure 9b shows the transition zone of the crack, in which it passes from a morphology characterized by streaks to a morphology characterized by dimples. The brittle crack region (Fig. 9b) includes microscopic voids of various sizes and shallow dimples indicating the highly ductile nature of AISI 316L stainless steel.

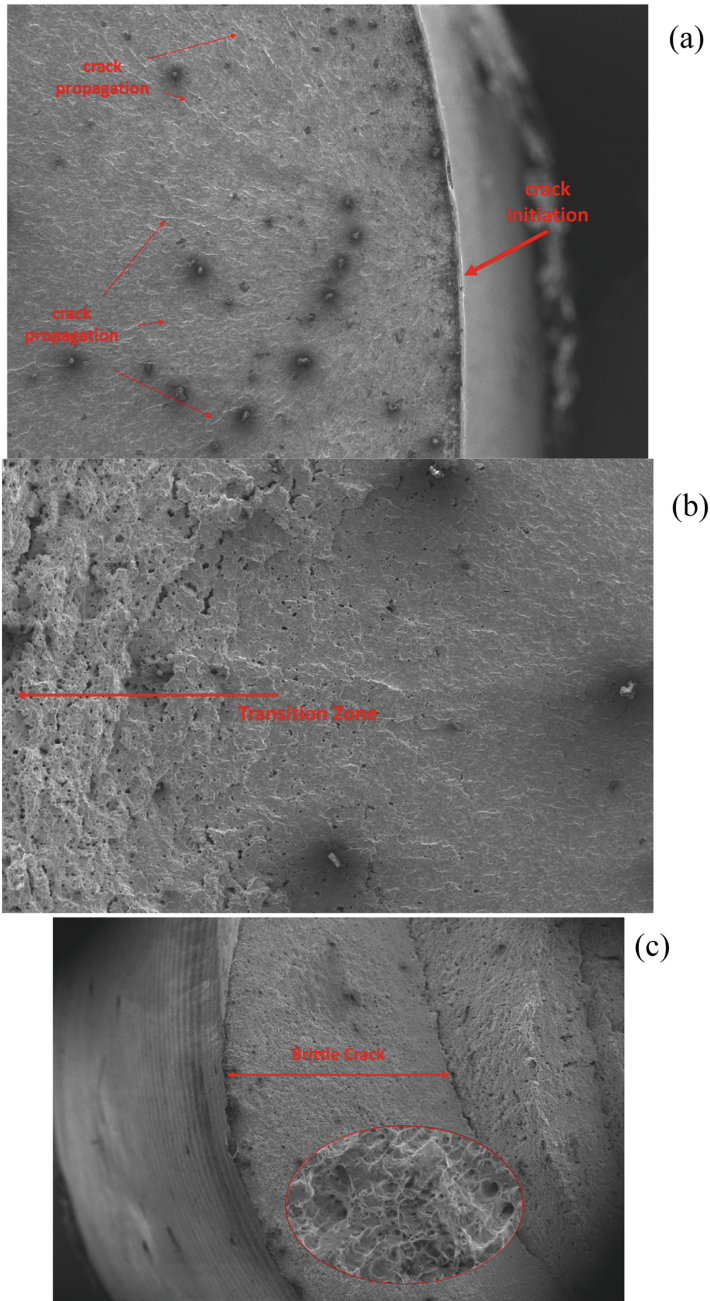


Fig. 9. SEM microscopies of AISI 316L fatigue fracture surface.

5 Conclusion

Static tensile and stepwise fatigue tests have been performed and the energy release of AISI 316L specimens has been monitored with an infrared camera.

The Static Thermographic Method (STM) allowed to assess a damage limit stress with rapid static tensile tests ($\sigma_{lim} = 282 \pm 15$ MPa), while the Risitano Thermographic Method (RTM) allowed to assess the fatigue limit with short-time stepwise fatigue tests ($\sigma_{0,RTM} = 274$ MPa for $R = -1$; $\sigma_{0,RTM} = 434$ MPa for $R = 0.1$). The previous values show good agreement with constant amplitude fatigue tests and literature data for the same material (-11% for the STM; -14% for the RTM respect Huang et al.).

The cyclic loading condition with stress ratio $R = -1$ is more damaging for the material, given the maximum applied stress level and testing frequency, compared to $R = 0.1$.

Even if several tests must be performed to compare the predicted values of limit stress by STM and fatigue limit by RTM, both for the two stress ratio conditions, the Thermographic Methods are able to assess in a very rapid way and with a limited number of specimens the first damage initiation within the material.

References

1. Curti, G., La Rosa, G., Orlando, M., Risitano, A.: Analisi tramite infrarosso termico della temperatura limite in prove di fatica. In: Proc XIV Convegno Naz AIAS, pp. 211–220 (1986)
2. Meneghetti, G.: Analysis of the fatigue strength of a stainless steel based on the energy dissipation. *Int. J. Fatigue* **29**, 81–94 (2007). <https://doi.org/10.1016/j.ijfatigue.2006.02.043>
3. Geraci, A., La Rosa, G., Risitano, A.: L'infrarosso termico nelle applicazioni meccaniche. In: CRES Symposium, Catania Italy, pp. 8–9 (1984)
4. La Rosa, G., Risitano, A.: Thermographic methodology for rapid determination of the fatigue limit of materials and mechanical components. *Int. J. Fatigue* **22**, 65–73 (2000). [https://doi.org/10.1016/S0142-1123\(99\)00088-2](https://doi.org/10.1016/S0142-1123(99)00088-2)
5. Pitarresi, G., Cappello, R., Catalanotti, G.: Quantitative thermoelastic stress analysis by means of low-cost setups. *Opt. Lasers Eng.* **134**, 106158 (2020). <https://doi.org/10.1016/j.optlaseng.2020.106158>
6. Vergani, L., Colombo, C., Libonati, F.: A review of thermographic techniques for damage investigation in composites. *Frat ed Integrita Strutt* **8**, 1–12 (2014). <https://doi.org/10.3221/IGF-ESIS.27.01>
7. Crupi, V., Guglielmino, E., Risitano, G., Tavilla, F.: Experimental analyses of SFRP material under static and fatigue loading by means of thermographic and DIC techniques. *Compos. Part B Eng.* **77**, 268–277 (2015). <https://doi.org/10.1016/j.compositesb.2015.03.052>
8. Plekhov, O., Naimark, O., Semenova, I., et al.: Experimental study of thermodynamic and fatigue properties of submicrocrystalline titanium under high cyclic and gigacyclic fatigue regimes. *Proc. Inst. Mech. Eng. Part C J. Mech. Eng. Sci.* **229**, 1271–1279 (2014). <https://doi.org/10.1177/0954406214563738>
9. Pitarresi, G., Tumino, D., Mancuso, A.: Thermo-mechanical behaviour of flax-fibre reinforced epoxy laminates for industrial applications. *Materials (Basel)* **8**, 7371–7388 (2015). <https://doi.org/10.3390/ma8115384>
10. Foti, P., Santonocito, D., Ferro, P., et al.: Determination of fatigue limit by static thermographic method and classic thermographic method on notched specimens. *Procedia Struct. Integr.* **26**, 166–174 (2020). <https://doi.org/10.1016/j.prostr.2020.06.020>

11. Meneghetti, G., Ricotta, M., Atzori, B.: A synthesis of the push-pull fatigue behaviour of plain and notched stainless steel specimens by using the specific heat loss. *Fatigue Fract. Eng. Mater. Struct.* **36**, 1306–1322 (2013). <https://doi.org/10.1111/ffe.12071>
12. Meneghetti, G., Ricotta, M.: The heat energy dissipated in the material structural volume to correlate the fatigue crack growth rate in stainless steel specimens. *Int. J. Fatigue* **115**, 107–119 (2018). <https://doi.org/10.1016/j.ijfatigue.2018.07.037>
13. Risitano, A., Risitano, G.: Determining fatigue limits with thermal analysis of static traction tests. *Fatigue Fract. Eng. Mater. Struct.* **36**, 631–639 (2013). <https://doi.org/10.1111/ffe.12030>
14. Corigliano, P., Cucinotta, F., Guglielmino, E., et al.: Fatigue assessment of a marine structural steel and comparison with Thermographic Method and Static Thermographic Method. *Fatigue Fract. Eng. Mater. Struct.* **43**, 734–743 (2020). <https://doi.org/10.1111/ffe.13158>
15. Risitano, G., Guglielmino, E., Santonocito, D.: Evaluation of mechanical properties of polyethylene for pipes by energy approach during tensile and fatigue tests. In: *Procedia Structural Integrity*, pp. 1663–1669. Elsevier B.V. (2018)
16. Cucinotta, F., D’Aveni, A., Guglielmino, E., et al.: Thermal emission analysis to predict damage in specimens of high strength concrete. *Frat ed Integrita Strutt* **15**, 258–270 (2021). <https://doi.org/10.3221/IGF-ESIS.55.19>
17. Ricotta, M., Meneghetti, G., Atzori, B., et al.: Comparison of experimental thermal methods for the fatigue limit evaluation of a stainless steel. *Metals (Basel)* **9**, 677 (2019). <https://doi.org/10.3390/met9060677>
18. Santonocito, D., Gatto, A., Risitano, G.: Energy release as a parameter for fatigue design of additive manufactured metals. *Mater. Des. Process Commun.* **3**, 1–7 (2021). <https://doi.org/10.1002/mdp2.255>
19. Fargione, G., Geraci, A., La Rosa, G., Risitano, A.: Rapid determination of the fatigue curve by the thermographic method. *Int. J. Fatigue* **24**, 11–19 (2002). [https://doi.org/10.1016/S0142-1123\(01\)00107-4](https://doi.org/10.1016/S0142-1123(01)00107-4)
20. Clienti, C., Fargione, G., La Rosa, G., et al.: A first approach to the analysis of fatigue parameters by thermal variations in static tests on plastics. *Eng. Fract. Mech.* **77**, 2158–2167 (2010). <https://doi.org/10.1016/j.engfracmech.2010.04.028>
21. Stamm, H., Holzwarth, U., Boerman, D.J., et al.: Effect of laser surface treatment on high cycle fatigue of AISI 316L stainless steel. *Fatigue Fract. Eng. Mater. Struct.* **19**, 985–995 (1996). <https://doi.org/10.1111/j.1460-2695.1996.tb01034.x>
22. Huang, H.W., Wang, Z.B., Lu, J., Lu, K.: Fatigue behaviors of AISI 316L stainless steel with a gradient nanostructured surface layer. *Acta Mater.* **87**, 150–160 (2015). <https://doi.org/10.1016/j.actamat.2014.12.057>
23. Roland, T., Reirant, D., Lu, K., Lu, J.: Fatigue life improvement through surface nanostructuring of stainless steel by means of surface mechanical attrition treatment. *Scr. Mater.* **54**, 1949–1954 (2006). <https://doi.org/10.1016/j.scriptamat.2006.01.049>
24. Peng, Y., Liu, Z., Chen, C., et al.: Effect of low-temperature surface hardening by carburization on the fatigue behavior of AISI 316L austenitic stainless steel. *Mater. Sci. Eng. A* **769**, 138524 (2020). <https://doi.org/10.1016/j.msea.2019.138524>